J Biochem **127**, 771–778 (2000)

Sequence Motif-Specific Assignment of Two [2Fe-2S] Clusters in Rat Xanthine Oxidoreductase Studied by Site-Directed Mutagenesis[1]

Toshio Iwasaki,[*,2] Ken Okamoto,[*,2] Tomoko Nishino,[*,†] Junko Mizushima,[*] Hiroyuki Hori,[*] and Takeshi Nishino[*,3]

[*]*Department of Biochemistry and Molecular Biology, Nippon Medical School, Sendagi, Tokyo 113-8602, and* [†]*Department of Biochemistry, Yokohama City University, School of Medicine, Fukuura, Yokohama 236-0004*

Received December 27, 1999, accepted February 10, 2000

The sequence motif-specific assignment of the two distinct [2Fe-2S] clusters in rat xanthine oxidoreductase (XOR) was unequivocally established by site-directed mutagenesis of recombinant enzymes expressed in a baculovirus-insect cell system and electron paramagnetic resonance (EPR) spectroscopy. The conserved cysteine residues, including Cys-115, in the unusual C-terminal -Cys-Xaa$_2$-Cys-//-Cys-Xaa$_1$-Cys- motif serve as ligands to the Fe/S I center, which is probably located in close proximity to the Mo-pterin center. Other conserved cysteine residues, including Cys-43 and Cys-51, in the N-terminal plant ferredoxin-like motif serve as ligands to the Fe/S II center, which is distantly located from the Mo-pterin center. The present sequence motif-specific assignment of the Fe/S I and II centers is discussed in the light of the structural features of XOR.

Key words: electron paramagnetic resonance spectroscopy, iron-sulfur cluster, site-directed mutagenesis, xanthine dehydrogenase, xanthine oxidase.

Xanthine oxidoreductase (XOR), xanthine dehydrogenase (XDH, EC 1.1.1.204) and xanthine oxidase (XO, EC 1.2.3.2), catalyzes the oxidation of xanthine to uric acid with concomitant reduction of NAD^+ or molecular oxygen (*1–4*). It is a homodimer of molecular weight 300,000, with each subunit having one non-covalently bound FAD, one molybdopterin-bound mononuclear molybdenum (Mo) center, and two $[2Fe\text{-}2S]^{2+,1+}$ clusters, and is the most extensively characterized member of the mononuclear molybdenum (Mo)-containing hydroxylase family (*1–7*). The reduction and oxidation reactions of the catalytic cycle of XOR are spatially separated: oxidative hydroxylation of xanthine to uric acid takes place at the Mo center in the 90-kDa molybdenum domain, and reducing equivalents thus introduced into enzymes are transferred rapidly *via* intramolecular electron transfer to FAD in the 40-kDa flavin domain, where physiological oxidation occurs (*2–4*). For this reason, intramolecular electron transfer between the Mo center and FAD center is an integral aspect of the overall catalytic sequence of this complex flavo-metalloprotein, and it has been extensively studied (*2–4*).

The two [2Fe-2S] clusters (Fe/S I and II) in the 20-kDa iron-sulfur (Fe/S) domain of XOR are indistinguishable in terms of the visible absorption spectra, but the midpoint redox potential of the Fe/S II center is ~80 mV more positive than that of the Fe/S I center (*8*, *9*), and their electron paramagnetic resonance (EPR) properties can be distinguished by their different g values and their different saturation properties at various temperatures (*10*, *11*). The Fe/S I center exhibits a rhombic EPR signal (g = 2.02, 1.93, and 1.90 ± 0.01), which is similar to those observed in the regular plant-type [2Fe-2S] ferredoxins and is readily observable at temperatures up to 40 K. On the other hand, the Fe/S II center exhibits an unusually broad EPR signal (g = 2.10 ± 0.02, 1.98 ± 0.015, and 1.91 ± 0.01), which is characteristic of some Mo-containing hydroxylases and can be observed only below 22 K. It should be noted that these EPR signals can be commonly observed in XOR and the related mononuclear Mo-containing hydroxylases with two [2Fe-2S] clusters [(*1*, *4*) and references therein].

The primary structures of the Fe/S domain of some mononuclear Mo-containing hydroxylases such as XOR (*12*, *13*) and *Desulfovibrio gigas* aldehyde oxidoreductase (AOR) (*14*) show the presence of eight strictly conserved cysteine residues (Fig. 1). These residues were recently shown to serve as ligands to the two [2Fe-2S] clusters in the *D. gigas* AOR structure [PDB entry, 1ALO.pdb (*15*)]. The N-terminal half of the Fe/S domain contains four of them, which are arranged to form the canonical [2Fe-2S] cluster binding motif of the regular plant-type ferredoxins (*3*, *4*, *12–15*). The C-terminal half contains the other four, which are arranged in the unusual -Cys-Xaa$_2$-Cys-//-Cys-Xaa$_1$-Cys- motif in a unique protein fold that is uniquely found in this enzyme family (*3*, *4*, *12–15*).

[1] This investigation was supported in part by a Grant-in-Aid for Scientific Research on Priority Areas "Biometalics" from the Ministry of Education, Science, Sports and Culture of Japan (08249104 to T. N.), and Grants-in-Aid from the Ministry of Education, Science, Sports and Culture of Japan (09480167 to T. N., 08770092 and 10770054 to K. O., and 8780599, 11169237, and 11780455 to T. I.).

[2] Contributed equally to this paper.

[3] To whom correspondence should be addressed. Phone: +81-3-3822-2131 (Ext 5216), Fax: +81-3-5685-3054, E-mail: nishino@nms.ac.jp

Abbreviations: AFR, activity/flavin ratio; AOR, aldehyde oxidoreductase; DCPIP, 2,6-dichlorophenolindophenol, EPR, electron paramagnetic resonance; Fe/S, iron-sulfur; g_{av}, the average g-factor; *Sf9*, *Spodoptera frugiperda*; XDH, xanthine dehydrogenase; XO, xanthine oxidase; XOR, xanthine oxidoreductase.

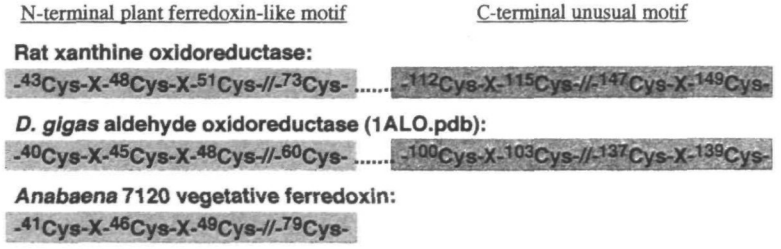

Fig 1. **Schematic representation of the two [2Fe-2S] cluster binding motifs in the Fe/S domain of rat XOR (*12*) and D. gigas AOR (*14*) [PDB entry, 1ALO.pdb (*15*)], and the plant-type ferredoxin motif of *Anabaena* 7120 vegetative ferredoxin (*22*, *41*).** Only conserved and potential cysteine ligand residues are shown

Although the sequence motif-specific assignment of the two [2Fe-2S] clusters to the corresponding EPR signals will greatly enhance our understanding of the structure-function relation in XOR, this remains controversial and is not conclusively established (reviewed in Ref. *4*). One possible approach to elucidate this problem is the combined application of site-directed mutagenesis and EPR spectroscopy, as has been successfully utilized for assignment of potential ligand residues to Fe/S cluster(s) in some Fe/S proteins with unknown structure and for analysis of the modified spectroscopic and/or redox properties of a particular redox site in some metalloproteins (*16–28*). However, the unavailability of an efficient heterologous expression system for XOR has been problematic in the past studies. In this paper, we unambiguously establish the sequence motif-specific assignment of the two [2Fe-2S] clusters in recombinant rat liver XOR, taking advantage of the baculovirus-insect cell (*Sf9*) expression system described elsewhere (*29*). Our results are discussed in the light of the structural features of XOR. Preliminary accounts of the present work have appeared in abstract form (*29*, *30*).

EXPERIMENTAL PROCEDURES

Materials—*Spodoptera frugiperda* (*Sf9*) cells and autographa california nuclear polyhedrosis virus (AcNPV) DNA were purchased from Novagen. The baculovirus transfer vector pJVP10Z (*31*) was a kind gift from Dr. Taylor (University of California, San Diego). Synthetic oligonucleotides were purchased from SCI-MEDIA (Tokyo). The culture medium IPL-41 for the *Sf9* cells was purchased from GIBCO BRL (Tokyo). DE-52 was obtained from Whatman, Bio-Gel HTP from Bio-Rad, and TSK-SW3000XL gel filtration column from Tosoh (Tokyo). Water was purified by the Milli-Q purification system (Millipore). Other chemicals used in this study were of analytical grade.

DNA Manipulations and Site-Directed Mutagenesis—The baculovirus-insect cell (*Sf9*) expression system (*29*) was employed for the expression of the wild-type XOR and single-point mutant enzymes. The site-directed mutagenesis was done by using a Muta-Gene Phagemid *in vitro* mutagenesis kit (Bio-Rad). All of the altered DNA sequences were analyzed by using a Sequenase ver. 2.0 DNA sequencing kit (United States Biochemical).

Escherichia coli strain CJ236 (Bio-Rad) was transformed with pUC119NX7 carrying the cDNA of rat liver XOR (*29*), and this transformant in the mid-log phase was infected with helper phage M13KO7 (Bio-Rad) in the presence of ampicillin, chloramphenicol, and kanamycin to prepare single-stranded DNA. The phage particles were collected by polyethyleneglycol precipitation, and the single-stranded DNA was extracted with phenol-chloroform and recovered by ethanol precipitation. The following 5′-phosphorylated DNA oligomer was utilized to construct the XOR variants: 5′-TGC CAG GAG TAC TGA ACC CAC ACT G-3′ for C115S (Cys-115 codon substituted by Ser codon); 5′-GGC TGT GGG GCA AGT ACT GTG ATG ATC-3′ for C51S (Cys-51 codon substituted by Ser codon); 5′-GAT CAT CAC GGT GGC TGC CCC ACA GCC-3′ for C51A (Cys-51 codon substituted by Ala codon); and 5′-ACA GCC ACC TTC TCC GGA GCC AAG CTT GGT CCC-3′ for C43S (Cys-43 codon substituted by Ser codon). Each oligonucleotide was hybridized to the single-stranded pUC119NX7 and introduced into *E. coli* strain HB101 (TAKARA, Tokyo). The resultant double-stranded vectors were isolated and digested with *Not*I and *Xba*I. Each obtained fragment was ligated with pRXD203 that had been digested with the same restriction enzymes, and each DNA fragment encoding mutant enzyme was excised by *Nhe*I and ligated into the baculovirus transfer vector pJVP10Z. The direction of the cDNA was identified by DNA sequencing.

Expression of XOR and Its Variants Using the Baculovirus-Insect Cell System and Purification of XOR—Coinfection with AcNPV DNA and constructed transfer vectors was conducted by using a Bac Vector 2000 (Novagen), and the screening of the recombinant virus was carried out by plaque assay according to the manufacturer's manual. The recombinant dimeric and monomeric enzymes were routinely produced and purified by following the color and/or the xanthine-O_2 and xanthine-NAD^+ oxidoreductase activities of the enzymes (*29*).

Rat liver XOR was purified as described previously (*32*). The recombinant wild-type enzymes utilized for the spectroscopic analysis in this paper were demolybdo forms of XOR. They were obtained after passing through a folate-affinity column chromatography to remove trace amounts of the molybdo dimer, which were quantitatively insufficient for the EPR analysis. The mutant enzymes C51S and C115S were unstable and partially purified by DEAE cellulose (DE-52) column chromatography to remove paramagnetic contaminants from the host insect cells. The mutant enzyme C43S was more stable than C51S and C115S, and the monomeric and dimeric forms of C43S were separated by hydroxylapatite column chromatography (*29*).

Analytical Methods—Absorption spectra were recorded using a Hitachi U3210 spectrophotometer. EPR measurements were carried out using a JEOL JEX-RE1X spectrometer equipped with an Air Products model LTR-3 Heli-Tran cryostat system, in which the temperature was monitored with a Scientific Instruments series 5500 temperature indicator/controller as reported previously (*33*). The EPR spectral data were processed using the KaleidaGraph software ver. 3.05 (Abelbeck Software) and the IgorPro ver. 3.02 (WaveMetrics). Preliminary EPR simulation was performed

using the WIN-EPR SimFonia software (written by Dr. Ralph T. Weber, Bruker Instruments, Billerica, MA) and the EPRSim XOP (PPC) for IgorPro software (written by Dr. John Boswell, Oregon Graduate Institute). Spin quantitation was estimated by double integration of EPR signals.

XOR concentration was determined from the absorbance at 450 nm using an extinction coefficient of 35.8 mM^{-1} cm^{-1} (*34*) for the native enzyme. The extinction coefficients at 450 nm of 32.6 and 23 mM^{-1} cm^{-1} (determined on the basis of FAD content after acid precipitation) were utilized for demolybdo-dimeric and demolybdo-monomeric XORs, respectively (Nishino, T., Amaya, Y., Kawamoto, S., Kashima, Y., Okamoto, K., Iwasaki, T., and Nishino, T., manuscript in preparation).

Xanthine-2,6-dichlorophenolindophenol (DCPIP) oxidoreductase activity was determined at 25°C by monitoring the absorption change at 600 nm in 50 mM potassium phosphate buffer, pH 7.8, containing 0.4 mM EDTA, 0.15 mM xanthine, and 50 μM DCPIP, in a final volume of 3.0 ml. An activity/flavin ratio (AFR) value of XOR was determined at 25°C (*32*), and fully active enzyme from rat liver was estimated to have an AFR value of 200 (*32*). The multiple sequence alignments were performed using the CLUSTAL X graphical interface (*35*) with small manual adjustments.

RESULTS AND DISCUSSION

The recombinant rat liver XOR produced by using the baculovirus-insect cell (*Sf9*) expression system was a heterogeneous mixture of the molybdo (native) dimeric, demolybdo dimeric, and demolybdo monomeric forms (*29*). Purification of each form of the recombinant XOR has been reported (*29*), and the properties of each form will be described in detail elsewhere. Although the molybdo XOR can be obtained after the folate affinity column chromatography, the amount and the stability of the recombinant wild-type and mutant enzymes are not enough to permit the usage of the molybdo form in EPR experiments. In the following EPR analysis, we therefore utilized the purified demolybdo or partially purified mixture in some experiments (see "EXPERIMENTAL PROCEDURES"). This does not affect the sequence motif-specific assignment of the two [2Fe-2S] clusters in XOR as described below.

EPR Spectra of the Recombinant Wild-Type XOR Dimer—Figure 2 shows the EPR spectra of dithionite-reduced molybdo and demolybdo dimeric XOR recorded at 16–39 K. The native molybdo dimeric XOR prepared from rat liver (traces A and B) exhibited a rhombic EPR signal at g = 2.02, 1.93, and 1.90 attributed to the Fe/S I center (observable at 39 K), in addition to overlapping broad rhombic resonance at g = 2.11, ~2.00, and ~1.90 attributed to the Fe/S II center. These EPR properties are essentially identical to those reported for milk XOR (*10*, *11*).

The purified recombinant wild-type demolybdo dimer of XOR contained ~8Fe/2FAD (mol/mol), indicating the presence of two [2Fe-2S] clusters per protomer (*29*), and showed no activity with xanthine and DCPIP as substrates, due to the absence of the Mo-pterin center (*2*). It elicited broad new resonances at g ~ 2.06 and 1.85, in addition to the signals attributed to the Fe/S I and II centers (Fig. 2, C and D). The relaxation behavior of the new g ~ 2.06 and 1.85 resonances is similar to that of the S = 1/2 EPR signal attributed to the Fe/S I center (Fig. 2, A and C), and these signals can be observed at 39 K, where the EPR signal attributed to the Fe/S II center is saturated and not observable. This suggests that the additional EPR features observed in the recombinant demolybdo dimeric enzyme cannot be attributed to the splitting of the EPR signal of the Fe/S I center due to magnetic interaction between the Fe/S I and II centers. Preliminary theoretical simulation and spin integrations also suggested that the g = 2.02 signal and the g = 2.06 signal are present approximately in a 1:1 ratio at 16 K and 39 K (data not shown). These results indicate that the Fe/S I site in the recombinant demolybdo dimeric enzyme is heterogeneous due to the absence of the Mo-pterin center and probably exists in (at least) two different forms and/or states in a ~1:1 ratio, whereas the Fe/S II site remains homogenous. It should be noted that the same observation has been reported with the fully demolybdo form of bovine milk XO (*36*). We suggest that the presence of the g = 2.02 signal and the additional g = 2.06 signal in a ~1:1 ratio is characteristic of demolybdo-dimeric XOR. Although the EPR signal of the Fe/S II center interferes with the g = 2.06 signal at lower temperatures, the g = 2.02 signal of the recombinant wild-type demolybdo dimer is apparently more intense in the first-derivative spectrum, and is therefore used as a diagnostic of the Fe/S I center in the following analysis.

EPR Properties of C115S Mutant Enzyme—In order to

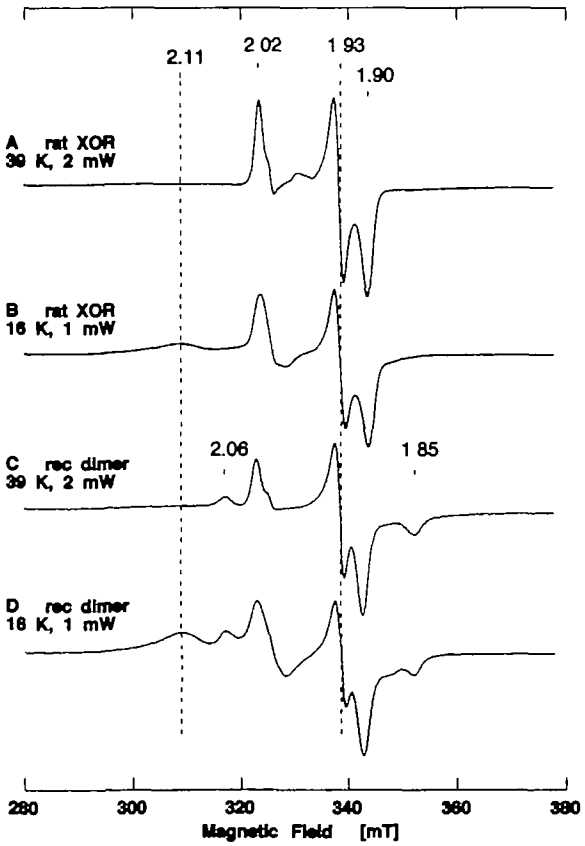

Fig. 2. **EPR spectra of the dithionite-reduced form of native XOR from rat liver (A, B) and recombinant wild-type XOR dimer (C, D).** Instrument settings for the X-band EPR spectroscopy. the temperature and microwave power are indicated in the figure; modulation amplitude, 0.79 millitesla. The g values are indicated in the figure

assign the Fe/S I and II centers in the recombinant demolybdo dimeric XOR, a mutant enzyme C115S, having a single amino acid replacement of Cys-115 by Ser, was constructed and expressed by using the baculovirus-insect cell expression system (*29*). The dimeric form of the resultant mutant enzyme C115S was rather unstable during purification under auxogenic conditions. Hence, the EPR spectra of dithionite-reduced C115S were recorded shortly after fractionation of the recombinant enzyme from the cell lysate by DEAE cellulose column chromatography (Fig. 3, C–F). The partially purified C115S was a mixture of monomeric and dimeric forms with a typical ratio of A_{450} and A_{550} of ~4.7 (varied from preparation to preparation) The negligible activity/flavin ratio (AFR) value (0.1) and specific xanthine-DCPIP oxidoreductase activity of 2.8–5.1 mol/min/mol of FAD (less than 0.5–1% of native enzyme) suggested that it is predominantly the demolybdo form (*32*). The control EPR experiment with the reduced recombinant wild-type enzyme from the same purification step confirmed little interference by other paramagnetic contaminants from the host insect cells in the $g = 2$ region under the applied conditions (data not shown).

EPR analysis of several different batches of partially purified C115S mutant enzyme in the reduced state showed that every batch contained a novel $[2Fe\text{-}2S]^{1+}$ center with near axial symmetry centered at $g = 1.92$ (Fig. 3, C and E), in addition to the broad EPR signal characteristic of the Fe/S II center at $g = 2.11$ that is indistinguishable from that of the recombinant wild-type dimeric enzyme (Fig. 3, A and C). The near-axial EPR signal at $g = 1.92$ is considerably broadened at 39 K (Fig. 3D). On the other hand, no rhombic EPR signal at $g = 2.02$, 1.93, 1.90 (the average g-factor, $g_{av} = 1.95$) characteristic of the Fe/S I center of the wild-type dimer (Fig. 3A) could be detected in any C115S preparation examined (Fig. 3, C–E). These data suggest that Cys-115 is one of the cysteine ligands of the Fe/S I center in the dimeric enzyme, and that the serine residue (Ser-115) serves as a non-cysteinyl ligand of this [2Fe-2S] cluster in the mutant enzyme C115S (Fig. 3, C–E). A similar EPR spectral change has been reported for the Cys-49→Ser mutation of the *Anabaena* vegetative ferredoxin, which also shows the near-axial EPR signal similar to those of the vertebrate-type ferredoxins and affects primarily the Fe(III) site of the [2Fe-2S] cluster (*22*). It should be noted, however, that Cys-115 of rat XOR is located in the unusual [2Fe-2S] cluster binding motif, -Cys-Xaa$_2$-Cys-//-Cys-Xaa$_1$-Cys-, at the C-terminal part of the Fe/S domain, with unique protein folding (*4*, *12*, *15*) (Fig. 1).

EPR Properties of C51S Mutant Enzyme—The N-terminal part of the Fe/S domain has the -Cys-Xaa$_4$-Cys-Xaa$_2$-Cys-//-Cys- motif, which is characteristically observed in regular plant-type ferredoxins (Fig. 1). A mutant enzyme C51S, having a single amino acid replacement of Cys-51 in the N-terminal motif with serine, was constructed and expressed by using the baculovirus-insect cell expression system. Like C115S, the resulting mutant enzyme C51S was rather unstable during purification under auxogenic conditions. Hence, the EPR spectra of dithionite-reduced C51S were recorded shortly after fractionation of the mutant enzyme from the cell lysate by DEAE cellulose column chromatography (Fig. 4). The partially purified C51S was a mixture of monomeric and dimeric forms with a typical ratio of A_{450} and A_{550} of ~4.4. The AFR value of 1.6 and the negligible xanthine-DCPIP oxidoreductase activity (2.8 mol/min/mol of FAD; less than 0.5% of native enzyme) suggested that it is predominantly the demolybdo form (*32*).

The EPR signals attributed to the $[2Fe\text{-}2S]^{1+}$ clusters in partially purified C51S are complicated due to the presence of both dimeric and monomeric forms (Fig. 4, C and D), and are very similar to the sum of the spectra of the recombinant wild-type dimer and monomer (Fig. 4B).

Although no change in the EPR signal attributed to the Fe/S I center was observed in crude C51S at 16 K and 39 K (Fig. 4, C and D), the resulting mutant enzyme was more unstable than the recombinant wild-type enzyme, as indi-

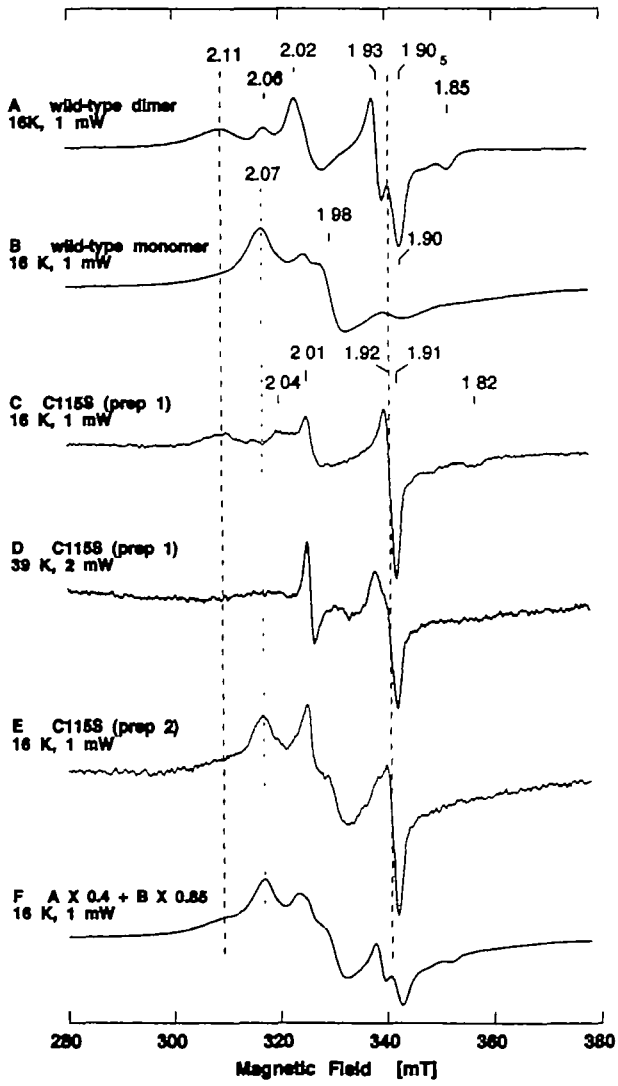

Fig. 3 **EPR spectra of the dithionite-reduced form of recombinant wild-type dimer (A) and monomer at 16 K (B), and partially purified C115S mutant enzyme at 16 K (C, E) and 39 K (D).** The near-axial EPR signal at $g = 1.92$ in the spectra C–E cannot be simulated as the sum of the spectra of the recombinant wild-type dimer and monomer (F) The EPR properties of recombinant wild-type dimer (A) and monomer at 16 K (B) are substantially different, and the details of the spectroscopic properties of the recombinant wild-type monomer will be reported elsewhere. Instrument settings for the EPR spectroscopy microwave power, 1 mW for A, B, C, E, and 2 mW for D; modulation amplitude, 0.79 millitesla The g values are indicated in the figure.

cated by faster bleaching of the brown color (data not shown). Unlike the wild-type enzyme (Fig. 5, A and B), further purification of crude C51S preparations under aerobic conditions resulted in marked loss of the [2Fe-2S] clusters in both the dimeric and monomeric forms, giving rather featureless EPR signals with a very poor signal-to-noise ratio (Fig. 5, C–E). Because the Cys→Ser mutants of *Anabaena* 7120 vegetative ferredoxin have been reported to be less stable than the wild-type ferredoxin (as expected from the relative pK_a values of cysteine and serine) (*22*), the instability of the clusters in C51S is likely to be due to the single amino acid replacement of Cys-51 by serine, which serves as a non-cysteinyl ligand of the [2Fe-2S] cluster (*i.e.*, the Fe/S II center) in partially purified C51S (Figs. 4 and 5).

We also constructed and expressed the C51A mutant enzyme, having a single amino acid replacement of Cys-51 with alanine, by using the baculovirus-insect cell expression system. Although the expression of the recombinant mutant enzyme was confirmed by Western blot analysis, the product was mostly obtained as an insoluble material (data not shown). This suggests that Cys-51 is a ligand residue with structural importance in protein conformation and/or folding.

EPR Properties of C43S Mutant Enzyme—In contrast to the C51S and C51A mutant enzymes described above, the mutant enzyme C43S, which has a single amino acid replacement of Cys-43 with serine in the N-terminal plant ferredoxin-like -Cys-Xaa$_4$-Cys-Xaa$_2$-Cys-//-Cys- motif (Fig. 1), was sufficiently stable to allow separation of the dimeric and monomeric forms from each other by gel filtration column chromatography. The dimeric form of C43S had a typical ratio of A_{450} and A_{550} of ~3.8 [estimated to contain ~1.8 [2Fe-2S] centers per FAD (mol/mol)], with the AFR value of ~2 and the negligible xanthine-DCPIP oxidoreductase activity of 3.1 mol/min/mol of FAD (0.6% of native enzyme), suggesting predominantly the demolybdo form (*32*). The monomeric form of C43S, like the wild-type demolybdo-monomeric XOR, showed no activity with xanthine and DCPIP as substrates.

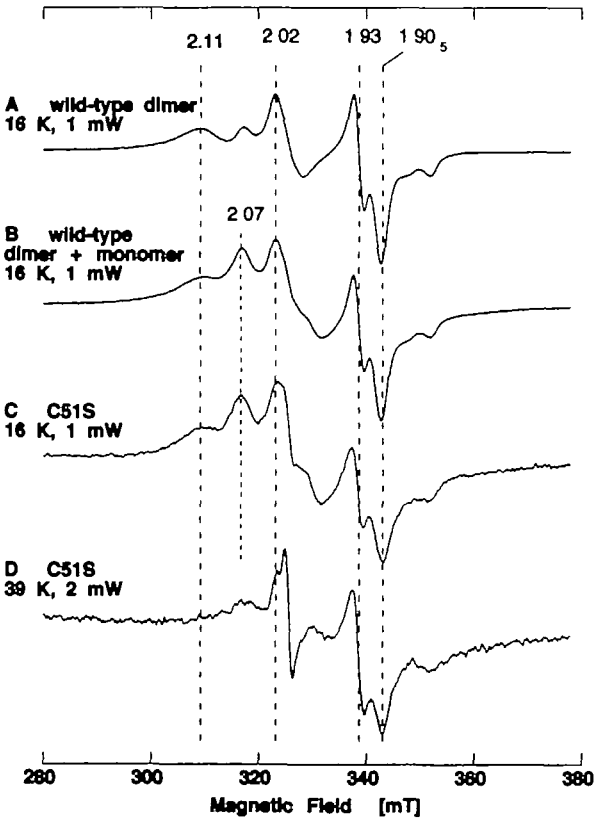

Fig. 4 **EPR spectra of the dithionite-reduced form of recombinant wild-type dimer at 16 K (A), and partially purified C51S mutant enzyme at 16 K (C) and 39 K (D).** The EPR spectrum C could be simulated as the sum of the spectra of the wild-type dimer and monomer (B). Instrument settings for the EPR spectroscopy: microwave power, 1 mW for A–C, and 2 mW for D; modulation amplitude, 0.79 millitesla. The *g* values are indicated in the figure.

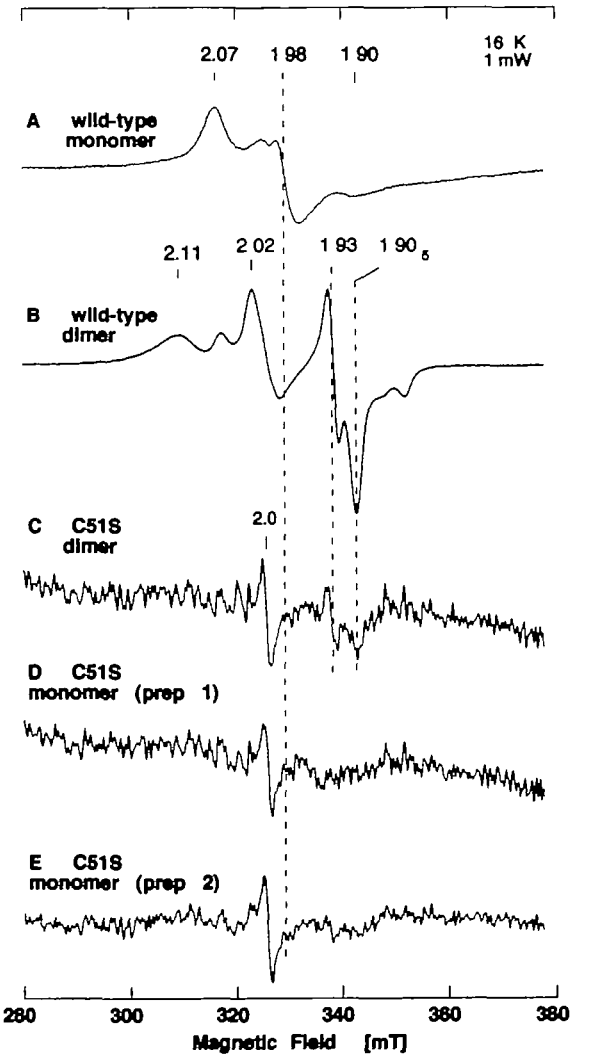

Fig. 5. **EPR spectra of the dithionite-reduced form of recombinant wild-type monomer (A), wild-type dimer (B), purified C51S dimer (C), and purified C51S monomer (D, E).** Purified C51S mutant enzyme preparations gave EPR spectra with a relatively poor signal-to-noise ratio, because of the instability of the bound [2Fe-2S] cluster after purification. Instrument settings for the EPR spectroscopy: temperature, 16 K; microwave power, 1 mW; modulation amplitude, 0.79 millitesla. The *g* values are indicated in the figure

The EPR spectra of the dimeric and monomeric forms of the dithionite-reduced C43S were substantially different from those of the recombinant wild-type demolybdo XOR (Fig. 6). The EPR spectra of the C43S dimer at 8–60 K clearly showed the presence of two overlapping S = 1/2 [2Fe-2S]$^{1+}$ clusters with different relaxation behaviors (Fig. 7). The EPR lineshape attributed to the Fe/S I center in C43S was essentially indistinguishable from that in the recombinant wild-type dimer (g_{av} = 1.95) (Fig. 7, A and E), whereas the signal attributed to the Fe/S II center was markedly modified, exhibiting a near-axial type signal at g = 2.05, ~1.94, ~1.93 (g_{av} ~ 1.97) (Fig. 7F). These data unequivocally showed that Ser-43 serves as a non-cysteinyl ligand of the Fe/S II center in the plant-type ferredoxin subdomain in the C43S dimer, without significant modification of the EPR lineshape attributed to the Fe/S I center. Interestingly, the effect of replacement of Cys-43→Ser in XOR, which results in the reduced Fe/S II center with g_{av} of ~1.97, is considerably different from that of the equivalent mutation (Cys-41→Ser) in reduced *Anabaena* 7120 vegetative ferredoxin, which results in the cluster with the lower g_{av} of ~ 1.92 (*22*).

Sequence Motif-Specific Assignment of the Fe/S I and II Centers—The present work established the unequivocal sequence motif-specific assignment of the two [2Fe-2S] clusters in recombinant XOR. The conserved cysteines (including Cys-43 and Cys-51) in the N-terminal plant-type ferredoxin motif in the Fe/S domain serve as ligands of the Fe/S II center with unusual EPR properties, while the other conserved cysteines (including Cys-115) in the C-terminal unusual [2Fe-2S] protein fold motif serve as ligands of the Fe/S I center with typical EPR properties of plant-type ferredoxins. This assignment is unexpected, given the unusual EPR signal of the Fe/S II center and the unusual protein folding of the C-terminal subdomain in XOR and the related enzymes. It is unequivocally established that the unusual EPR features of the Fe/S II center in dimeric XOR are *not* due to a polypeptide fold or a cluster-binding sequence motif. The faster spin-lattice relaxation time of the Fe/S II center for a regular plant ferredoxin-type [2Fe-

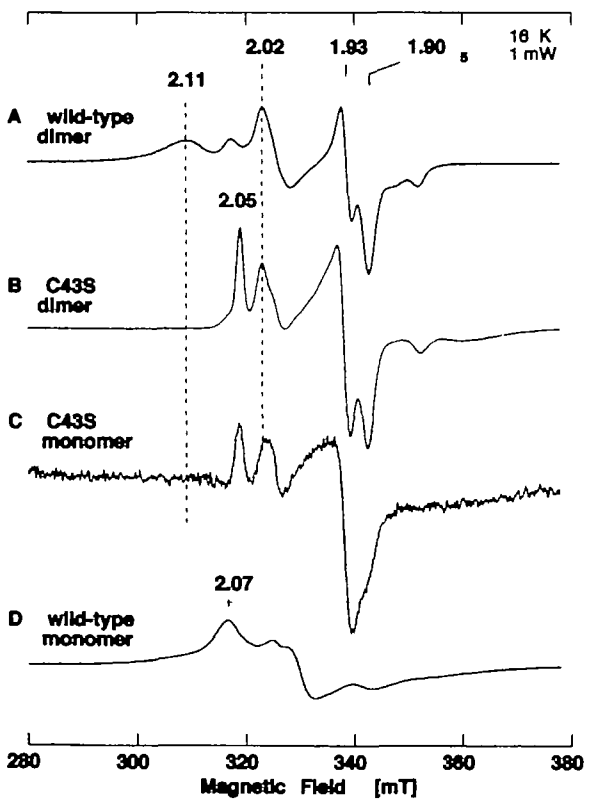

Fig 6. **EPR spectra of the dithionite-reduced form of recombinant wild-type dimer (A), dimeric C43S mutant enzyme (B), monomeric C43S mutant enzyme (C), and recombinant wild-type monomer (D).** Instrument settings for the EPR spectroscopy. temperature, 16 K; microwave power, 1 mW; modulation amplitude, 0 79 millitesla. The g values are indicated in the figure.

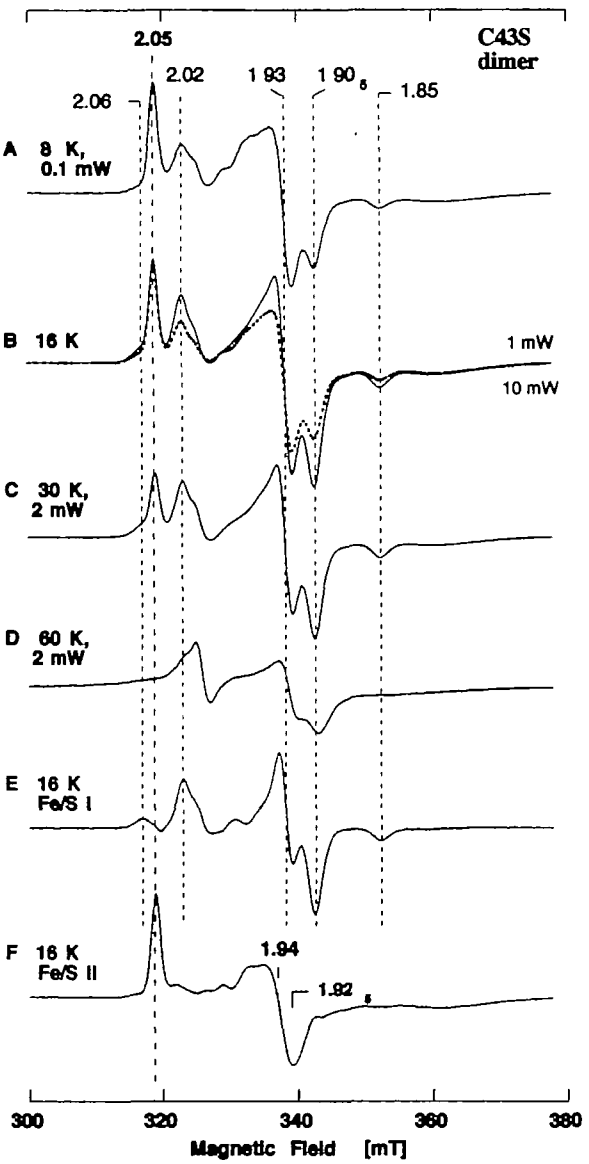

Fig 7. **EPR spectra of the dithionite-reduced form of purified dimeric C43S mutant enzyme at 8–60 K.** The spectra E and F were obtained by subtraction of the EPR spectra at 16 K recorded at the microwave power of 1 mW (B, solid trace) and 10 mW (B, dashed trace). Instrument settings for the EPR spectroscopy: modulation amplitude, 0 79 millitesla. The g values are indicated in the figure.

$2S]^{1+}$ cluster (*4*, *10*, *11*) and the *D. gigas* AOR structure (*15*) imply a possible relation to the solvent accessibility of the N-terminal plant ferredoxin subdomain and/or a magnetic interaction between the Fe/S I and Fe/S II centers.

It has been reported that the EPR signal attributed to the Fe/S I center of XOR and AOR interacts magnetically with the Mo center when the two sites are paramagnetic (*37*). In the X-ray crystal structure of *D. gigas* AOR (PDB entry, 1ALO.pdb), the crystallographic distance between the Mo center and the nearest [2Fe-2S] cluster bound to the C-terminal part of the Fe/S domain is ~12 Å (*15*), thus being consistent with our assignment. The EPR spectroscopic heterogeneity of the Fe/S I center in demolybdo XOR dimer (Fig. 2) may be attributed to the absence of the Mo center in the recombinant dimeric enzymes used in this work.

Finally, after completion of this work, the X-ray crystal structure of bovine milk XDH was solved and is being refined to 2.1 Å resolution (*38*) (Enroth, C., Eger, B.T., Pai, E.F., Okamoto, K., Nishino, T., and Nishino, T., manuscript in preparation). In conjunction with this three-dimensional structural information (*38*), the present sequence motif-specific assignment of the two [2Fe-2S] clusters in XOR indicates that the Fe/S I center is located in the vicinity of the Mo-pterin center, and the Fe/S II center in the vicinity of the FAD center. Hence, the sequence of the intramolecular electron transfer in XOR probably occurs as follows: Mo-pterin→Fe/S I→Fe/S II→FAD. During the preparation of this paper, the same conclusion was described with a bacterial XOR-related enzyme, CO dehydrogenase from *Oligotropha carboxidovorans* (*39*, *40*). These features may be common to several other XOR-related enzymes with similar cofactor arrangement and EPR properties as XOR.

We thank Drs K. Tamura, S. Oogami, and T. Iizuka (The Institute of Physical and Chemical Research) for allowing us to utilize the EPR facility.

REFERENCES

1. Hille, R. (1992) Xanthine oxidase, xanthine dehydrogenase, and aldehyde oxidase in *Chemistry and Biochemistry of Flavoenzymes* (Müller, F., ed.) Vol. III, pp. 21–68, CRC Press, Boca Raton, FL
2. Nishino, T. (1994) The conversion of xanthine dehydrogenase to xanthine oxidase and the role of the enzyme in reperfusion injury. *J. Biochem.* **116**, 1–6
3. Hille, R. and Nishino, T. (1995) Xanthine oxidase and xanthine dehydrogenase. *FASEB J.* **9**, 995–1003
4. Hille, R. (1996) The mononuclear molybdenum enzymes. *Chem. Rev.* **96**, 2757–2816
5. Bray, R.C. (1975) Molybdenum iron-sulfur flavin hydroxylases and related enzymes in *The Enzymes*, 3rd ed. (Boyer, P.D., ed.) Vol. XII, part B, pp. 299–419, Academic Press, New York
6. Hille, R. and Massey, V. (1985) Molybdenum-containing hydroxylase· xanthine oxidase, aldehyde oxidase, and sulfite oxidase in *Molybdenum Enzymes* (Spiro, T.G., ed.) Vol. 7, pp. 443–518, Wiley-Interscience, New York
7. Bray, R.C. (1988) The inorganic biochemistry of molybdoenzymes. *Q. Rev. Biophys.* **21**, 299–329
8. Porras, A.G. and Palmer, G. (1982) The room temperature potentiometry of xanthine oxidase· pH-dependent redox behavior of the flavin, molybdenum, and iron-sulfur centres. *J. Biol. Chem.* **257**, 11617–11626
9. Hunt, J., Massey, V., Dunham, W.R., and Sands, R.H. (1993) Redox potentials of milk xanthine dehydrogenase: room temperature measurement of the FAD and 2Fe/2S center potentials. *J. Biol. Chem.* **268**, 18685–18691
10. Palmer, G. and Massey, V. (1969) Electron paramagnetic resonance and circular dichroism studies on milk xanthine oxidase. *J. Biol. Chem.* **244**, 2614–2620
11. Hille, R., Hagen, W.R., and Dunham, W.R. (1985) Spectroscopic studies on the iron-sulfur centers of milk xanthine oxidase. *J. Biol. Chem.* **260**, 10569–10575
12. Amaya, Y., Yamazaki, K., Sato, M., Noda, K., Nishino, T., and Nishino, T. (1990) Proteolytic conversion of xanthine dehydrogenase from the NAD-dependent type to the O_2-dependent type. *J. Biol. Chem.* **265**, 14170–14175
13. Sato, A., Nishino, T., Noda, K., Amaya, Y., and Nishino, T. (1995) The structure of chicken liver xanthine dehydrogenase cDNA cloning and the domain structure. *J. Biol. Chem.* **270**, 2818–2826
14. Thoenes, U., Flores, O.L., Neves, A., Devreese, B., Van Beeumen, J.J., Huber, R., Romao, M.J., LeGall, J., Moura, J.J.G., and Rodrigues-Pousada, C. (1994) Molecular cloning and sequence analysis of the gene of the molybdenum-containing aldehyde oxido-reductase of *Desulfovibrio gigas* the deduced amino acid sequence shows similarity to xanthine dehydrogenase. *Eur. J. Biochem.* **220**, 901–910
15. Romão, M.J., Archer, M., Moura, I., Moura, J.J.G., LeGall, J., Engh, R., Schneider, M., Hof, P., and Huber, R. (1995) Crystal structure of the xanthine oxidase-related aldehyde oxido-reductase from *D. gigas*. *Science* **270**, 1170–1176
16. Werth, M.T., Cecchini, G., Manodori, A.M., Ackrell, B.A., Schröder, I., Gunsalus, R.P., and Johnson, M.K. (1990) Site-directed mutagenesis of conserved cysteine residues in *Escherichia coli* fumarate reductase: modification of the spectroscopic and electrochemical properties of the [2Fe-2S] cluster. *Proc. Natl. Acad. Sci. USA* **87**, 8965–8969
17. Martín, A.E., Burgess, B.K., Stout, C.D., Cash, V.L., Dean, D.R., Jensen, G.M., and Stephens, P.J. (1990) Site-directed mutagenesis of *Azotobacter vinelandii* ferredoxin I: [Fe-S] cluster-driven protein rearrangement. *Proc. Natl. Acad. Sci. USA* **87**, 598–602
18. Rothery, R.A. and Weiner, J.H. (1991) Alteration of the iron-sulfur cluster composition of *Escherichia coli* dimethyl sulfoxide reductase by site-directed mutagenesis. *Biochemistry* **30**, 8296–8305
19. Manodori, A., Cecchini, G., Schröder, I., Gunsalus, R.P., Werth, M.T., and Johnson, M.K. (1992) [3Fe-4S] to [4Fe-4S] cluster conversion in *Escherichia coli* fumarate reductase by site-directed mutagenesis. *Biochemistry* **31**, 2703–2712
20. Augier, V., Guigliarelli, B., Asso, M., Bertrand, P., Frixon, C., Giordano, G., Chippaux, M., and Blasco, F. (1993) Site-directed mutagenesis of conserved cysteine residues within the β subunit of *Escherichia coli* nitrate reductase: physiological, biochemical, and EPR characterization of the mutated enzymes. *Biochemistry* **32**, 2013–2023
21. Warren, P.V., Smart, L.B., McIntosh, L., and Golbeck, J.H. (1993) Site-directed conversion of cysteine-565 to serine in PsaB of photosystem I: results in the assembly of [3Fe-4S] and [4Fe-4S] clusters in Fx: a mixed-ligand [4Fe-4S] cluster is capable of electron transfer to F_A and F_B. *Biochemistry* **32**, 4411–4419
22. Cheng, H., Xia, B., Reed, G.H., and Markley, J.L. (1994) Optical, EPR, and ^1H NMR spectroscopy of serine-ligated [2Fe-2S] ferredoxins produced by site-directed mutagenesis of cysteine residues in recombinant *Anabaena* 7120 vegetative ferredoxin. *Biochemistry* **33**, 3155–3164
23. Meyer, J., Fujinaga, J., Gaillard, J., and Lutz, M. (1994) Mutated forms of the [2Fe-2S] ferredoxin from *Clostridium pasteurianum* with noncysteinyl ligands to the iron-sulfur cluster. *Biochemistry* **33**, 13642–13650
24. Crouse, B.R., Sellers, V.M., Finnegan, M.G., Dailey, H.A., and Johnson, M.K. (1996) Site-directed mutagenesis and spectroscopic characterization of human ferrochelatase· identification of residues coordinating the [2Fe-2S] cluster. *Biochemistry* **35**, 16222–16229
25. Xia, B., Cheng, H., Bandarian, V., Reed, G.H., and Markley, J.L.

(1996) Human ferredoxin overproduction in *Escherichia coli*, reconstitution *in vitro*, and spectroscopic studies of iron-sulfur cluster ligand cysteine-to-serine mutants. *Biochemistry* **35**, 9488–9495
26 Jung, Y.S., Vassiliev, I.R., Yu, J., McIntosh, L., and Golbeck, J.H. (1997) Strains of *Synechocystis* sp. PCC 6803 with altered PsaC: II. EPR and optical spectroscopic properties of F_A and F_B in aspartate, serine, and alanine replacements of cysteines 14 and 51. *J. Biol. Chem.* **272**, 8040–8049
27. Rousset, M., Montet, Y., Guighalelli, B., Forget, N., Asso, M., Bertrand, P., Fontecilla-Camps, J.C., and Hatchikian, E.C. (1998) [3Fe-4S] to [4Fe-4S] cluster conversion in *Desulfovibrio fructosovorans* [NiFe] hydrogenase by site-directed mutagenesis. *Proc. Natl. Acad. Sci. USA* **95**, 11625–11630
28. Sellers, V.M., Wang, K.F., Johnson, M.K., and Dailey, H.A. (1998) Evidence that the fourth ligand to the [2Fe-2S] cluster in animal ferrochelatase is a cysteine: characterization of the enzyme from *Drosophila melanogaster*. *J. Biol. Chem.* **273**, 22311–22316
29. Nishino, T., Kashima, Y., Okamoto, K., Iwasaki, T., and Nishino, T. (1997) The monomeric form of xanthine dehydrogenase expresses in baculovirus-insect cell system in *Flavins and Flavoproteins 1996* (Stevenson, K.J., Massey, V., and Williams, C.H. Jr., eds.) pp. 843–846, University of Calgary Press, Calgary
30. Okamoto, K., Iwasaki, T., Nishino, T., Hori, H., Mizushima, J., and Nishino, T. (1997) Properties of xanthine dehydrogenase that lacks iron-sulfur centers. *J. Inorg. Biochem.* **67**, 263
31. Kilpatrick, L.-T.K., Kennedy, M.C., Beinert, H., Czernuszewicz, R.C., Qiu, D., and Spiro, T.G. (1994) Cluster structure and H-bonding in native, substrate-bound, and 3Fe forms of aconitase as determined by resonance Raman spectroscopy. *J. Am. Chem. Soc.* **116**, 4053–4061
32. Ikegami, T. and Nishino, T. (1986) The presence of desulfo xanthine dehydrogenase in purified and crude enzyme preparations from rat liver. *Arch. Biochem. Biophys.* **247**, 254–260
33 Iwasaki, T., Wakagi, T., Isogai, Y., Tanaka, K., Iizuka, T., and Oshima, T. (1994) Functional and evolutionary implications of a [3Fe-4S] cluster of the dicluster-type ferredoxin from the thermoacidophilic archaeon, *Sulfolobus* sp. strain 7. *J. Biol. Chem.* **269**, 29444–29450
34 Johnson, J.L., Waud, W.R., Cohen, H.J., and Rajagopalan, K.V. (1974) Molecular basis of the biological function of molybdenum molybdenum-free xanthine oxidase from livers of tungsten-treated rats. *J. Biol. Chem.* **249**, 5056–5061
35. Thompson, J.D., Gibson, T.J., Plewniak, F., Jeanmougin, F., and Higgins, D.G. (1997) The CLUSTAL_X windows interface flexible strategies for multiple sequence alignment aided by quality analysis tools. *Nucleic Acids Res.* **25**, 4876–4882
36 Gardlik, S., Barber, M.J., and Rajagopalan, K.V. (1987) A molybdopterin-free form of xanthine oxidase. *Arch. Biochem. Biophys.* **259**, 363–371
37 Lowe, D.J. and Bray, R.C. (1978) Magnetic coupling of the molybdenum and iron-sulphur centres in xanthine oxidase and xanthine dehydrogenases. *Biochem. J.* **169**, 471–479
38. Enroth, C., Eger, B.T., Pai, E.F., Okamoto, K., Iwasaki, T., Nishino, T., Hori, H., and Nishino, T. (1999) Crystal structure of xanthine oxidoreductase and EPR assignment of Fe/S centers in *Flavins and Flavoproteins 1999* (Ghisla, S., Kroneck, P., Macheroux, P., and Sund, H., eds.) pp. 783–786, Agency for Scientific Publ., Berlin
39 Dobbeck, H., Gremer, L., Meyer, O., and Huber, R. (1999) Crystal structure and mechanism of CO dehydrogenase, a molybdo iron-sulfur flavoprotein containing S-selanylcysteine. *Proc. Natl. Acad. Sci. USA* **96**, 8884–8889
40. Gremer, L., Kellner, S., Meyer, O., Dobbek, H., and Huber, R. (1999) A new type of flavin adenine dinucleotide-binding resolved in the molybdo iron-sulfur-flavoprotein carbon monoxide dehydrogenase from *Oligotropha carboxidovorans* in *Flavins and Flavoproteins 1999* (Ghisla, S., Kroneck, P., Macheroux, P., and Sund, H., eds.) pp. 759–766, Agency for Scientific Publ., Berlin
41 Rypniewski, W.R., Breiter, D.R., Benning, M.M., Wesenberg, G., Oh, B.-H., Markley, J.L., Rayment, I., and Holden, H.M. (1991) Crystallization and structure determination to 2.5-Å resolution of the oxidized [2Fe-2S] ferredoxin isolated from *Anabaena* 7120. *Biochemistry* **30**, 4126–4131